Electronic Supplementary Material (ESI) for Dalton Transactions.

Interconnected hierarchical $NiCo_2O_4$ microspheres as high performance electrode material for supercapacitor

Ming Cheng,[a] Hongsheng Fan,[a] Yuanjun Song,[b] Yimin Cui,[a] and Rongming Wang*[b]

[a] Department of Physics, Beihang University, Beijing 100191, P. R. China

[b] Beijing Key Laboratory for Magneto-Photoelectrical Composite and Interface Science, School of Mathematics and Physics, University of Science and Technology Beijing, Beijing 100083, P. R. China

E-mail: rmwang@ustb.edu.cn

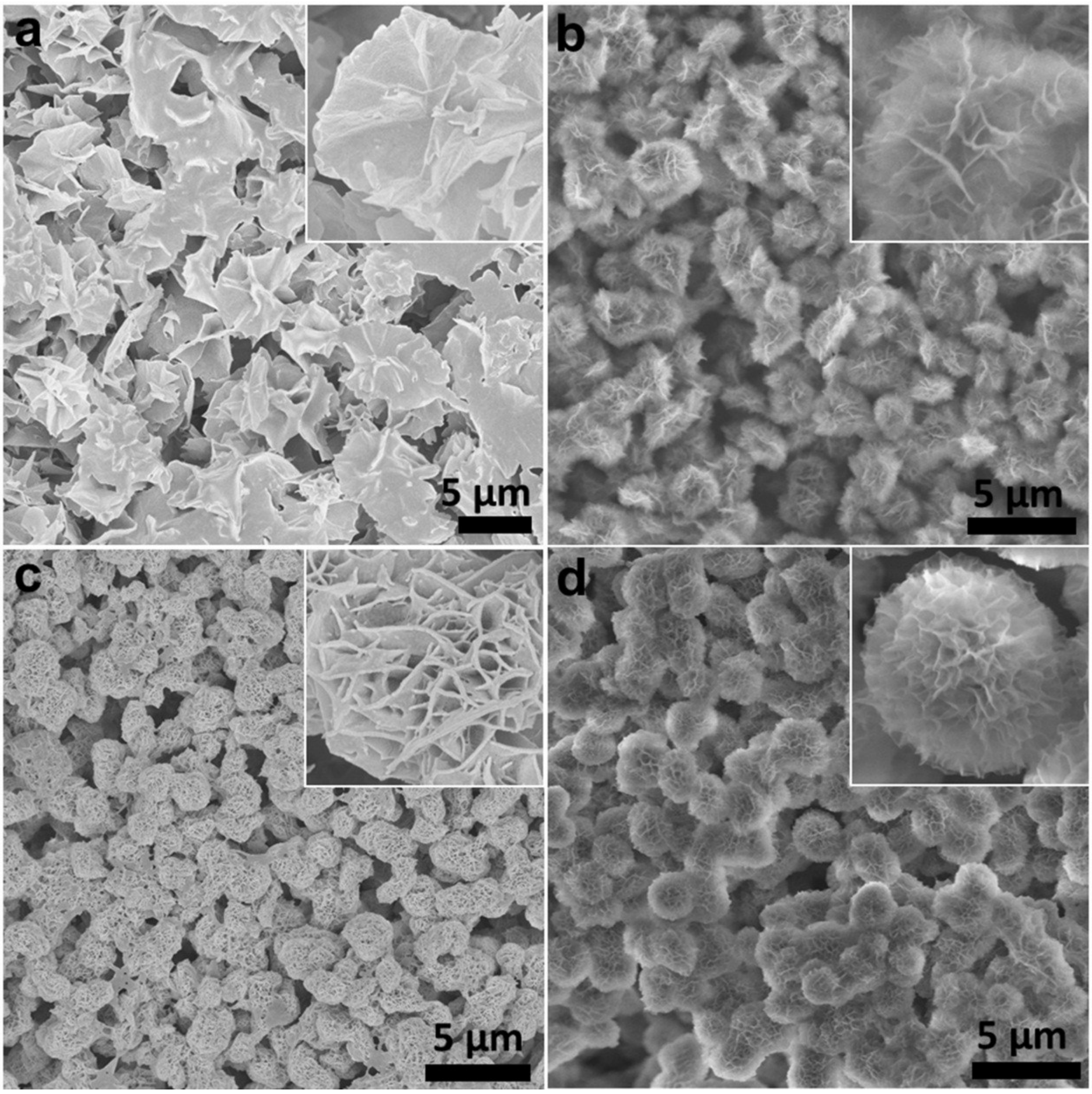

Fig. S1 Typical SEM images of the nickel-cobalt glycolate precursor synthesized with 1 mL deionized water and different amount of IPA and EG: (a) 40 mL IPA and 20 mL EG, (b) 35 mL IPA and 25 mL EG, (c) 30 mL IPA and 20 mL EG, (d) 25 mL IPA and 35 mL EG.

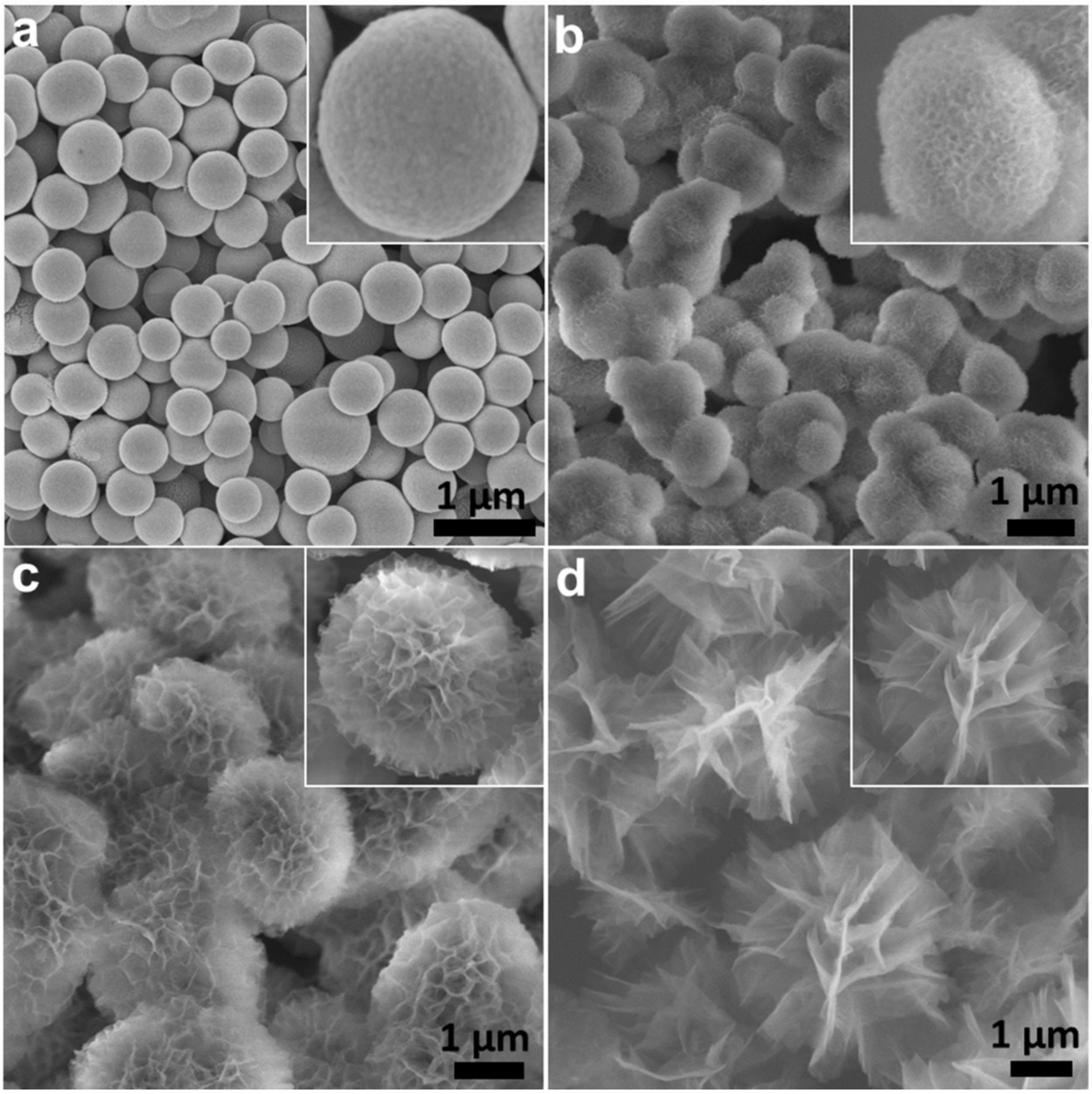

Fig. S2 Typical SEM images of the nickel-cobalt glycolate precursor synthesized with 25 mL IPA and 35 mL EG and different amount of deionized water: (a) 0 mL , (b) 0.5 mL, (c) 1 mL, (d) 1.5 mL.

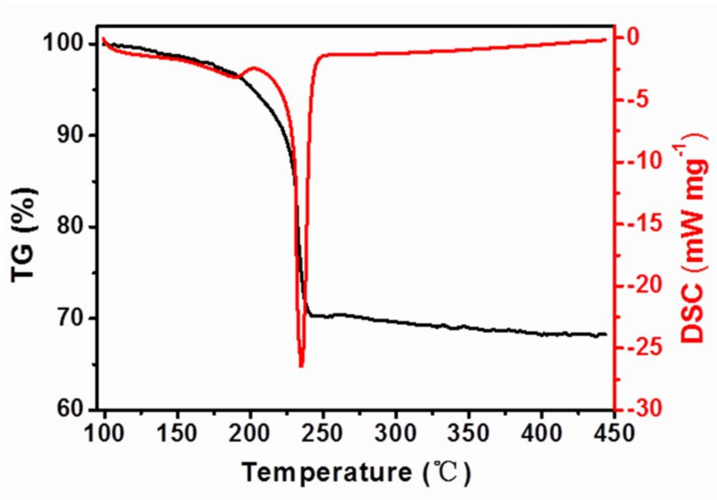

Fig. S3 TGA curves of the $NiCo_2O_4$ precursor.

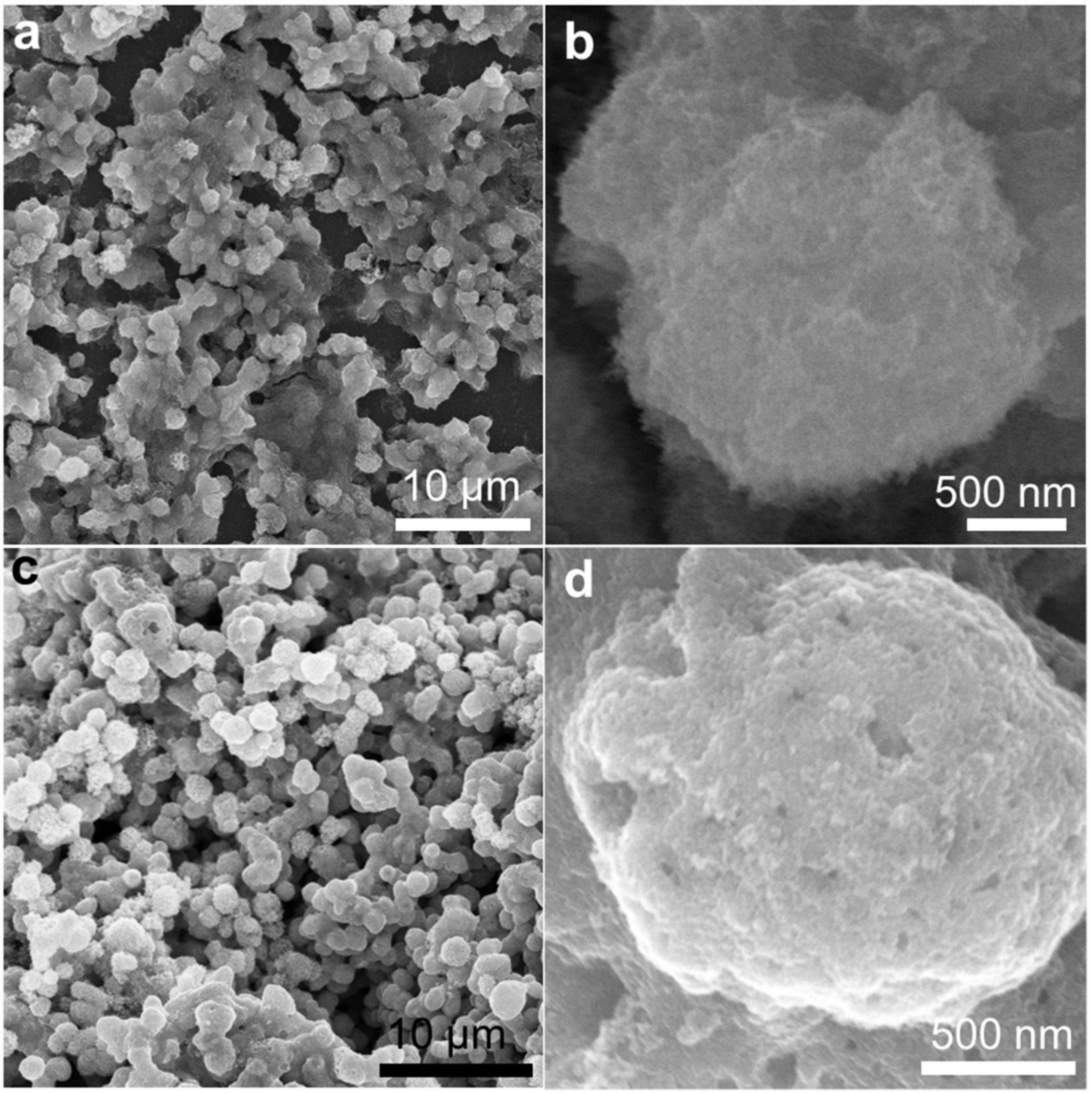

Fig. S4 SEM images of the obtained $NiCo_2O_4$ prouducts after calcined at in air at 250 °C (a,b) and 300 °C (c,d).

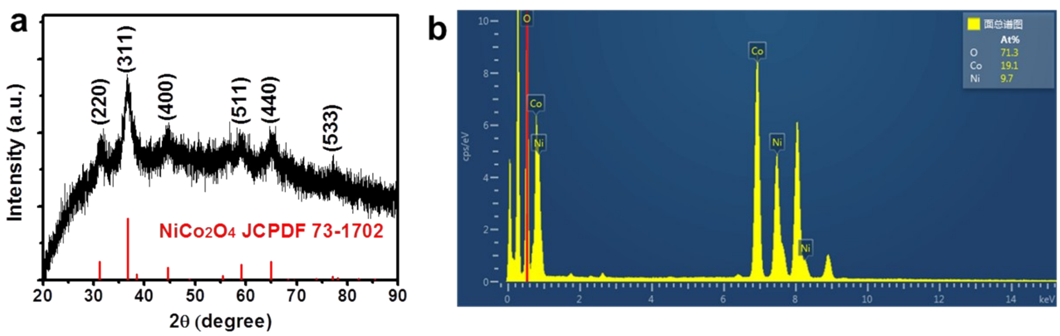

Fig. S5 XRD pattern (a) and EDS spectrum (b) of the IH-$NiCo_2O_4$ sample.

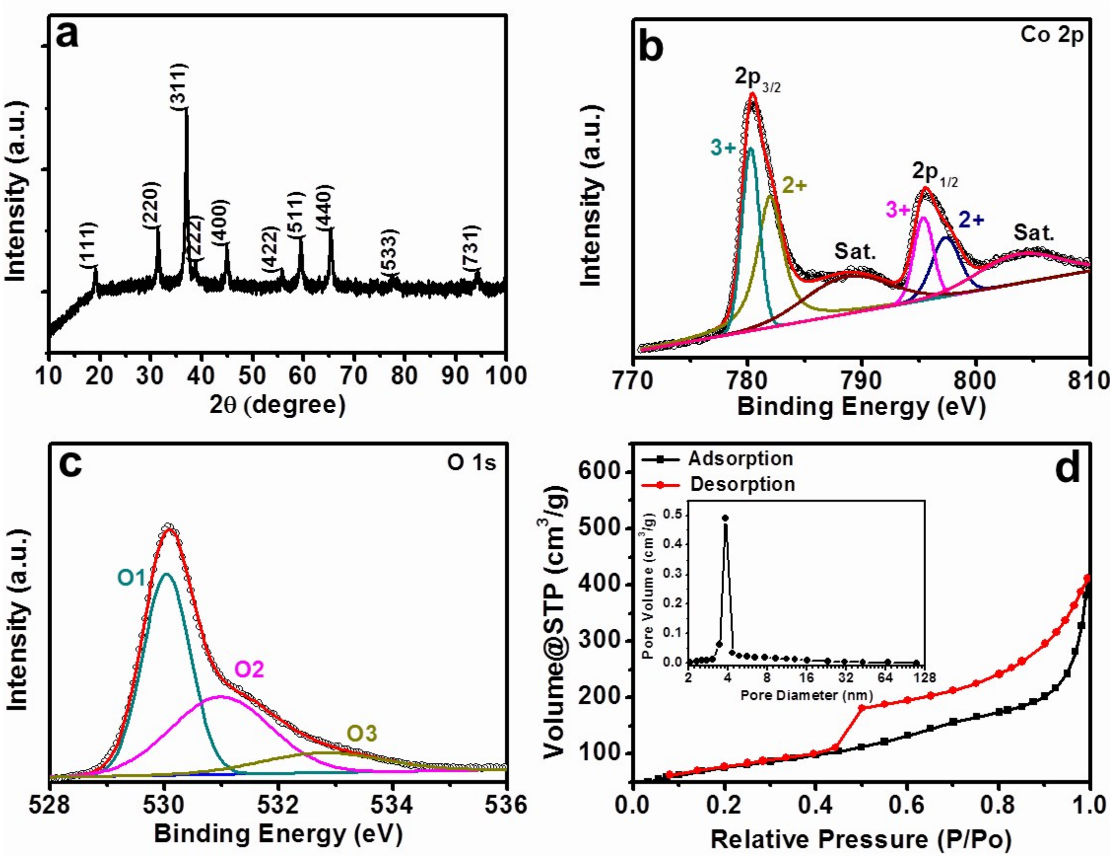

Fig. S6 (a) XRD pattern of the IH-Co_3O_4 sample. High resolution XPS spectra for the Co 2p (b) and O 1s (c) of the IH-Co_3O_4 sample. (d) Typical N_2 adsorption and desorption isotherms and the pore-size-distribution curves (inset) of the IH-Co_3O_4.

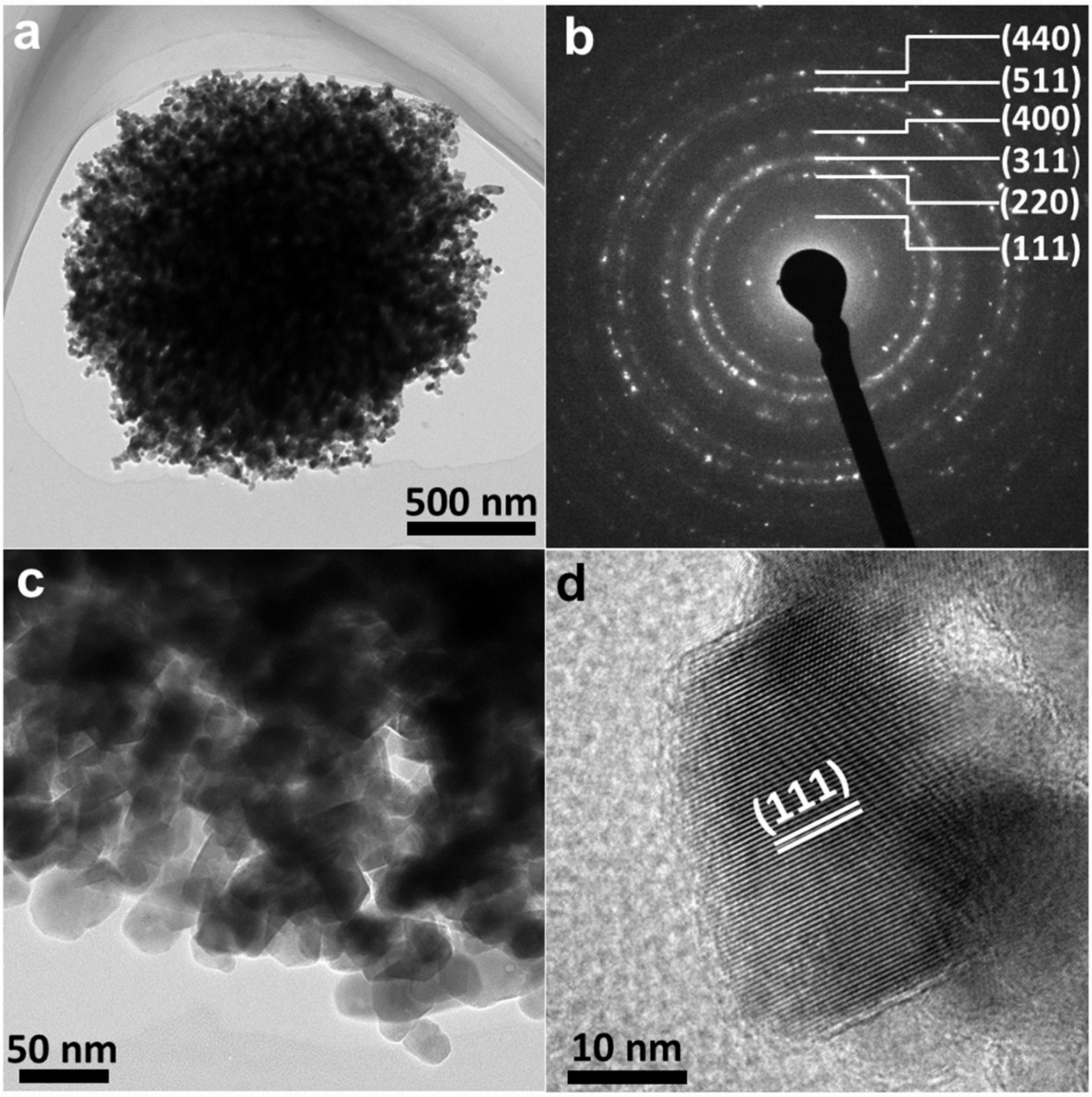

Fig. S7 TEM image (a) and corresponding SAED pattern (b) of an individual IH-Co_3O_4 microsphere. (c) TEM image of the local characteristic region of the IH-Co_3O_4 microsphere. (d) HRTEM lattice image of the IH-Co_3O_4 microsphere.

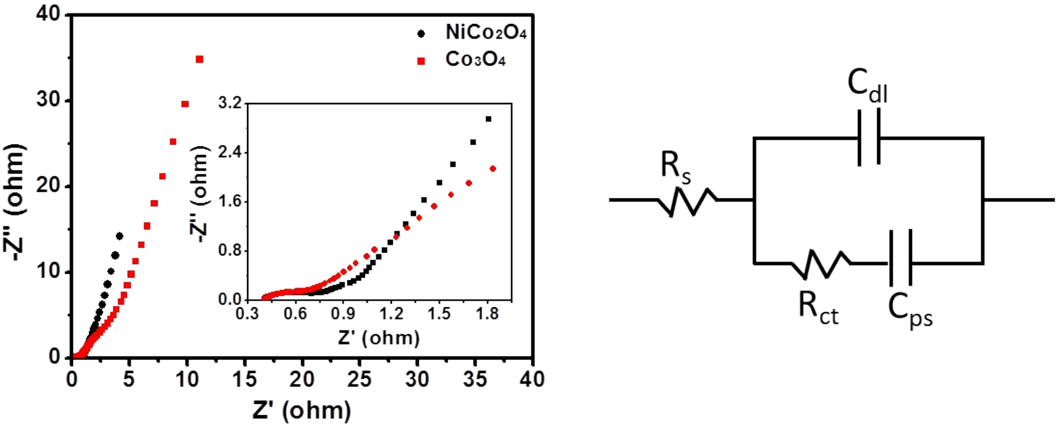

Fig. S8 EIS plots of the IH-$NiCo_2O_4$ and IH-Co_3O_4 and the equivalent circuit model for the EIS spectra.

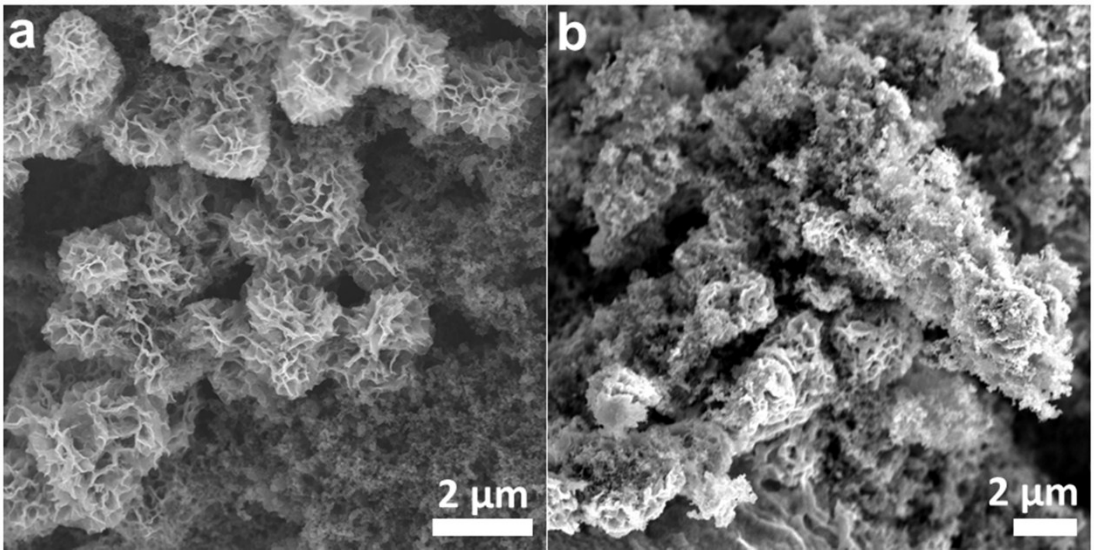

Fig. S9 SEM images of the IH-$NiCo_2O_4$ elecrode before (a) and after (b) 7000 cycles at a high current density of 10 g A^{-1}.

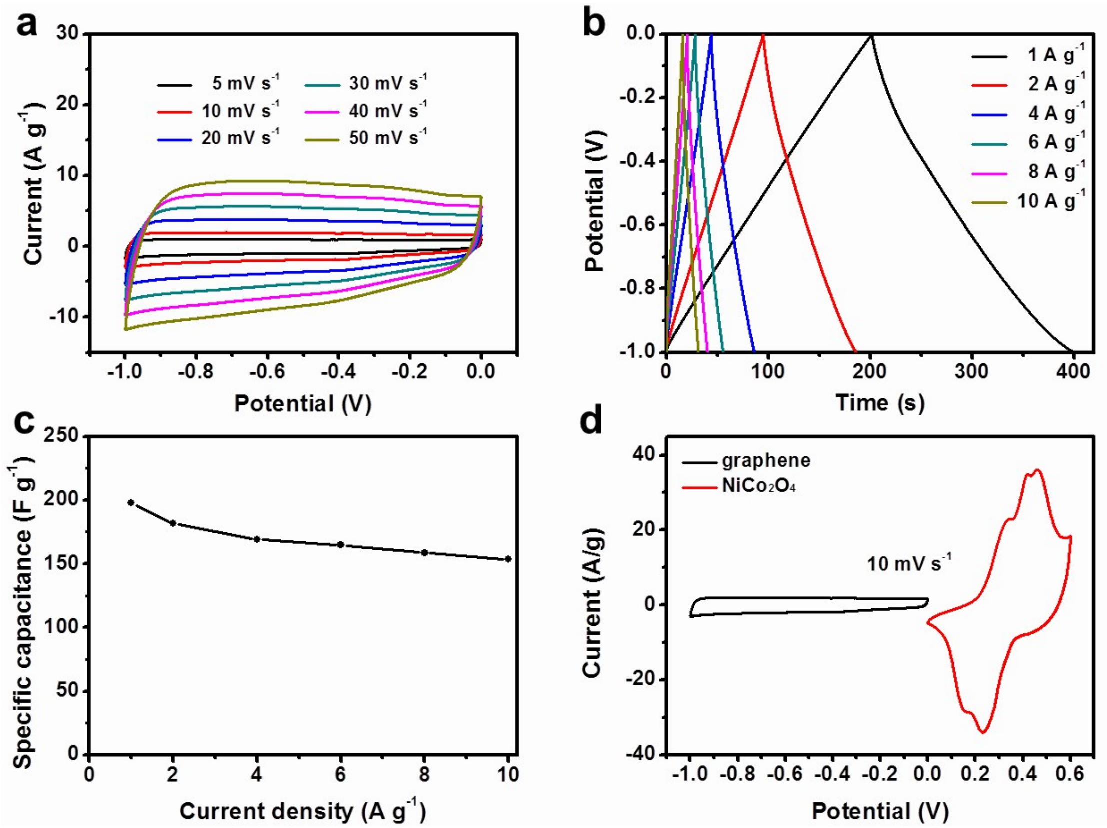

Fig. S10 CV curves at different scan rates (a) and charge-discharge curves at different current densities (b) of the graphene electrode. (c) The corresponding specific capacitances at different current densities of the graphene electrode. (d) Compared CV curves of the IH-$NiCo_2O_4$ and graphene at a scan rate of 10 mV s^{-1}.

Table S1 A comparison with previously reported $NiCo_2O_4$ nanomaterials.

Material	Morphology	Mass loading (mg cm^{-2})	Potential Window (V)	Specific capacitance@current density	Capacity retention (%)
Rambutan-like $NiCo_2O_4$[1]	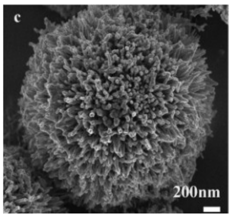	2.0	0-0.4	798 F g^{-1}@0.5 A g^{-1}	91.7(1500 cycles@2 A g^{-1})
Urchin like $NiCo_2O_4$[2]	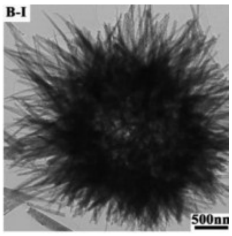	>1	0-0.45	658 F g^{-1}@1 A g^{-1}	98.4(1000 cycles@10 A g^{-1})
Hollow urchin-like $NiCo_2O_4$ microspheres[3]	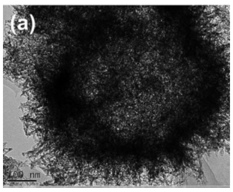	2.5-3.5	0-0.5	950 F g^{-1}@1 A g^{-1}	93.6(1500 cycles@6 A g^{-1})
Hollow $NiCo_2O_4$ sub-microspheres[4]	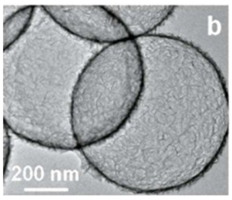	8	0-0.4	678 F g^{-1}@1 A g^{-1}	87(3500 cycles@10 A g^{-1})
Flower-like $NiCo_2O_4$ hierarchitectures[5]	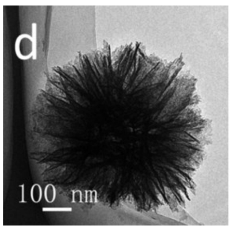	——	0-0.55	1191.2 F g^{-1}@1 A g^{-1}	78(1200 cycles@1 A g^{-1})
Spinel $NiCo_2O_4$ nanostructure[6]	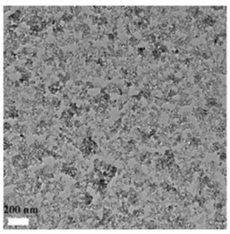	1	0-0.4	1362 F g^{-1}@1 A g^{-1}	41(1500 cycles@4 A g^{-1})
$NiCo_2O_4$ nanoflake composites[7]	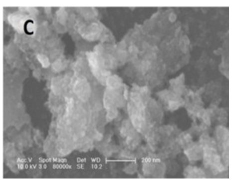	2	0-0.4	1468 F g^{-1}@4 A g^{-1}	85.5(5000 cycles@4 A g^{-1})

Nanowires buliding $NiCo_2O_4$ architectures[8]	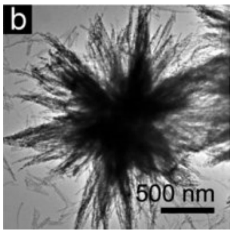	1.3	0-0.5	1080 F g^{-1}@2 A g^{-1}	86.5(1500 cycles@4 A g^{-1})
Nanosheets buliding $NiCo_2O_4$ architectures[8]	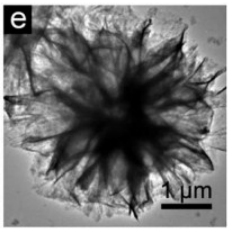	1.3	0-0.5	1400 F g^{-1}@5 A g^{-1}	94(1500 cycles@4 A g^{-1})
Nanorod-assembled $NiCo_2O_4$ hollow microspheres[9]	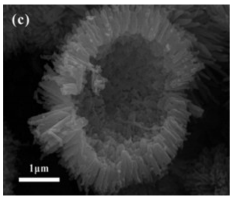	——	0-0.5	764 F g^{-1}@2 A g^{-1}	101.7(1500 cycles@2 A g^{-1})
$NiCo_2O_4$ nanosheets[10]	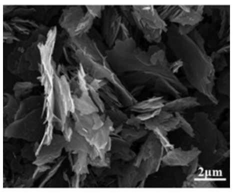	——	0-0.45	876 F g^{-1}@1 A g^{-1}	88(1000 cycles@1 A g^{-1})
Hierarchical mesoporous $NiCo_2O_4$ hollow nanocubes[11]	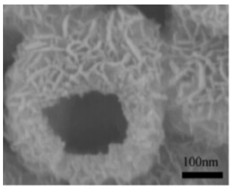	1	0-0.45	795.6 F g^{-1}@1 A g^{-1}	97.5(2000 cycles@1 A g^{-1}) 96.1(2000 cycles@2 A g^{-1})
Urchin like $NiCo_2O_4$[12]	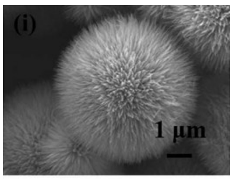	2.1	0-0.55	436.1 F g^{-1}@1 A g^{-1}	No decay(1000 cycles@10 A g^{-1})
Mesoporous $NiCo_2O_4$ nanospheres[13]	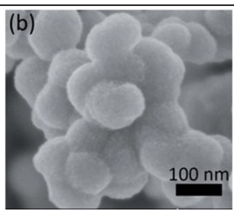	2	0-0.4	842 F g^{-1}@2 A g^{-1}	107(1000 cycles@30 mV s^{-1})
Multiple hierarchical $NiCo_2O_4$[14]	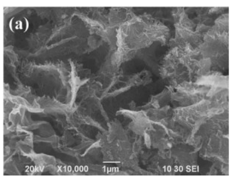	5.0-6.0	0-0.45	1393 F g^{-1}@ 0.5 A g^{-1}	——

Hierarchical $NiCo_2O_4$ tetragonal microtubes[15]	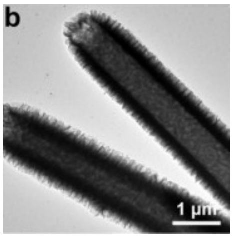	1.0	0-0.53	1387.9 F g^{-1}@2 A g^{-1}	89.4(12000 cycles@10 A g^{-1})
Hollow $NiCo_2O_4$ submicrospheres[16]	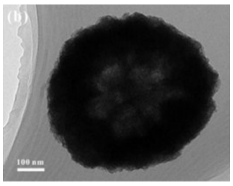	——	0-0.5	987 F g^{-1}@1 A g^{-1}	No decay(5000 cycles@5 A g^{-1})
$NiCo_2O_4$ double-shell hollow spheres[17]	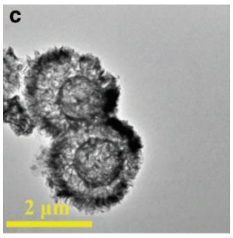	3.76	0-0.4	781 F g^{-1}@1 A g^{-1}	85.8(2000 cycles@2 A g^{-1})
Mesoporous $NiCo_2O_4$ nanosheets[18]	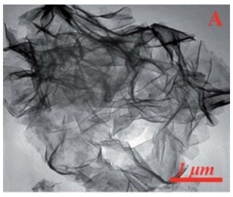	1	0-0.35	292 F g^{-1}@1 A g^{-1}	90(2000 cycles@8 A g^{-1})
3D network-like mesoporous $NiCo_2O_4$[19]	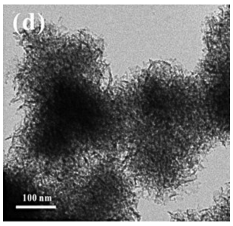	1.0	0-0.5	931 F g^{-1}@3 A g^{-1}	125.5(1000 cycles@3 A g^{-1})
IH-$NiCo_2O_4$ (This work)	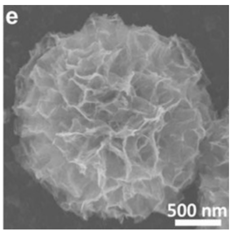	**2.1**	**0-0.55**	**1822.3 F g^{-1} @2 A g^{-1}**	**87.6(7000 cycles@10 A g^{-1})**

References

1. Y. Shang, Y. Gai, L. Wang, L. Hao, H. Lv, F. Dong and L. Gong, *Eur. J. Inorg.c Chem.*, 2017, **2017**, 2340.
2. J. Xiao and S. Yang, *RSC Adv.,* 2011, **1**, 588.
3. Y. Lei, Y. Wang, W. Yang, H. Yuan and D. Xiao, *RSC Adv.,* 2015, **5**, 7575.
4. C. Yuan, J. Li, L. Hou, J. Lin, G. Pang, L. Zhang, L. Lian and X. Zhang, *RSC Adv.*, 2013, **3**, 18573.
5. C. An, Y. Wang, Y. Huang, Y. Xu, C. Xu, L. Jiao and H. Yuan, *CrystEngComm*, 2014, **16**, 385.
6. S. Jiang, Y. Sun, H. Dai, P. Ni, W. Lu, Y. Wang, Z. Li and Z. Li, *Electrochim. Acta,* 2016, **191**, 364.
7. Y. Sun, X. Xiao, P. Ni, Y. Shi, H. Dai, J. Hu, Y. Wang, Z. Li and Z. Li, *Electrochim. Acta*, 2014, **121**,

270.
8. L. Yu, H. Wu, T. Wu and C. Yuan, *RSC Adv.*, 2013, **3**, 23709.
9. Y. Zhu, X. Ji, R. Yin, Z. Hu, X. Qiu, Z. Wu and Y. Liu, *RSC Adv.*, 2017, **7**, 11123.
10. L. Zhang, W. Zheng, H. Jiu, C. Ni, J. Chang and G. Qi, *Electrochim. Acta.,* 2016, **215**, 212.
11. C. Zheng, C. Cao, R. Chang, J. Hou and H. Zhai, *Phys. Chem. Chem. Phys.,* 2016, **18**, 6268.
12. J. Wang, Y. Zhang, J. Ye, H. Wei, J. Hao, J. Mu, S. Zhao and S. Hussain, *RSC Adv.*, 2016, **6**, 70077.
13. M. J. Pang, S. Jiang, G. H. Long, Y. Ji, W. Han, B. Wang, X. L. Liu, Y. L. Xi, F. Z. Xu and G. D. Wei, *RSC Adv.*, 2016, **6**, 67839.
14. S. Wang, S. Sun, S. Li, F. Gong, Y. Li, Q. Wu, P. Song, S. Fang and P. Wang, *Dalton T.*, 2016, **45**, 7469.
15. F.-X. Ma, L. Yu, C.-Y. Xu and X. W. Lou, *Energy Environ. Sci.*, 2016, **9**, 862.
16. Y. Zhu, J. Wang, Z. Wu, M. Jing, H. Hou, X. Jia and X. Ji, *J. Power Sources*, 2015, **287**, 307.
17. X. Li, L. Jiang, C. Zhou, J. Liu and H. Zeng, *NPG Asia Mater.*, 2015, **7**, e165.
18. S. Khalid, C. Cao, A. Ahmad, L. Wang, M. Tanveer, I. Aslam, M. Tahir, F. Idrees and Y. Zhu, *RSC Adv.*, 2015, **5**, 33146.
19. Y. Zhu, Z. Wu, M. Jing, W. Song, H. Hou, X. Yang, Q. Chen and X. Ji, *Electrochim. Acta*, 2014, **149**, 144.